

Effect of controlled environmental conditions on mechanical, microstructural and durability properties of cement mortar

Alireza Joshaghani^{a,*}, Mohammad Balapour^b, Ali Akbar Ramezaniapour^c

^aZachry Department of Civil Engineering, Texas A&M University, College Station, TX, USA

^bCAEE Department, Drexel University, Philadelphia, USA

^cConcrete Technology and Durability Research Center, Department of Civil Engineering, Amirkabir University of Technology, Tehran, Iran

HIGHLIGHTS

- Effect of temperature and relative humidity on durability properties.
- Use of thin sections method for investigating microstructure.
- Higher relative humidity improved the durability properties of mortar.
- Pearson correlation coefficient among test results was calculated.
- DC and the sorptivity results were strongly related.

ARTICLE INFO

Article history:

Received 12 September 2017

Received in revised form 10 December 2017

Accepted 27 December 2017

Keywords:

Temperature

Relative humidity

Dielectric constant (DC)

Shrinkage

Rapid chloride migration test (RCMT)

Sorptivity

Thin sections

ABSTRACT

Environmental conditions, such as temperature and relative humidity, impact the rate of evaporation, mechanical properties and durability of concrete. Thus, they have a direct effect on the development of transport properties. The purpose of this study is to investigate the effect of controlled environmental conditions on moisture retention, dielectric constant (DC), compressive strength, shrinkage, water sorptivity index, rapid chloride migration test (RCMT), microscopical analysis (thin sections) and electrical resistivity. The mortar specimens were prepared using Ordinary Portland Cement with two water-to-cement ratios of 0.42 and 0.52. The specimens cured in the controlled environments of 25, 46 and 65 °C for temperature, and 30% and 90% for relative humidity. The results showed that curing under higher temperature cause reduction in compressive strength and increase in the sorptivity index. Moreover, a great correlation between DC measurements and sorptivity, the RCMT and electrical resistivity was found. Higher relative humidity helped the performance of samples, considering the durability and mechanical properties.

© 2017 Elsevier Ltd. All rights reserved.

1. Introduction

It is well-known that environmental conditions, such as relative humidity and temperature, can have a great influence on both mechanical and especially durability-related properties of concrete, which control the final quality. One of the key factors that controls the concrete's quality is moisture evaporation through the concrete that can cause cracking, therefore reducing the durability of concrete in terms of service life. Thus, in order to optimize chemical reactions, providing a suitable temperature and relative humidity in the curing process seems necessary to prevent exces-

sive water loss through the surface of concrete during the hydration process [30,8,62]. During continuous evaporation on the surface of early-age concrete, a negative capillary pressure is built-up and continues to rise with the progress of moisture loss that causes surface tension forces, and eventually cracking [56]. Bakhshi et al. [15] with the use of a fluid-mechanic based approach, provided a model for the prediction of evaporation rate and concluded that an increase in the ambient temperature would lead to an extreme rate of water content evaporation in concrete that will be escalated by a decrease in ambient relative humidity and an increase in wind speed [25].

Determining the dielectric constant (DC) of concrete is a non-destructive test (NDT), which can show the water content of concrete in various stages. Basically, the DC is a material's physical characteristic that demonstrates its ability to store electrical

* Corresponding author at: 199 Spence St., Suite 508K DLEB, 3135 TAMU, College Station, TX, USA.

E-mail address: joshaghani@tamu.edu (A. Joshaghani).

energy. The DC of free water is 80.1 at 20 °C, which is considerably higher than solids, such as aggregate, cement and hydration products, which have a DC around 3–8. Therefore, a shift in the free water content in concrete can cause a change in DC values [23,57,66]. Water in concrete can be divided into three categories, including chemically bound water, physically bound water, and free water. Considering that chemical and physical water has a powerful molecular bond, their DC is not remarkable. Hence, a shift in free water content can affect DC and demonstrate the alteration of free water into chemically or physically bounded water, which is evidence of the continuous hydration process and consumption of free water over time. Shen et al. [55] stated that free water content is alluded to capillary pores at early ages, therefore DC can reflect the capillary pores. They also observed that there is a linear relationship between free water content DC. This method is excellent to determine water content in the fresh concrete mixture.

Chen et al. [23] observed a significant change in the DC value of the fresh concrete mix with the alteration in temperature. In fact, with an increase in temperature, the DC value will reduce owing to the fact that the higher temperature will help the evaporation of water from the surface of the concrete. They have also investigated the effect of the water-to-binder ratio (w/b) of fresh concrete from 0.45 to 0.57, which showed the increment in DC values with the growth in w/b. This enhancement in DC values can be explained by an increase in free water content, which was provided in the fresh concrete mix by an increase of w/b. The reduction of DC with an increase in temperature was also observed by Yehia et al. [70].

Several studies have been conducted on the effect of curing temperature on compressive strength, and the general conclusion was that the higher temperature leads to greater compressive strength values at early ages, but the concrete loses this compressive strength over time [59,65]. This matter can be explained by the fact that an increase of temperature will speed up the hydration process reactions at early ages and lead to the formation of a more C-S-H gel, and, as a result, greater values of compressive strength. But it should be noted that high temperature will cause a non-uniform distribution of C-S-H gel at long-term ages owing to inadequate time for diffusion through concrete, which contributes to larger pores in the microstructure of concrete and weaker mechanical and durability properties [5,73]. Atiş et al. [14] investigated the effect of both w/c and two relative humidity percentages of 65% and 100% on the compressive strength of concrete containing silica fume. They have reported that drying the curing condition can notably influence the compressive strength of concrete and it is more sensitive to this curing condition when the w/c increases. This matter can be explained by considering an enhancement in w/c led to the presence of greater porosity content and bigger capillary pores, thereby letting the free water to evaporate easily.

Generally, shrinkage may induce microcracking in the structure of concrete that can cause problems relating to the durability properties of concrete and lead to costly repairing implementations for enhancing the service life of concrete structures [71,33]. Autogenous shrinkage relates to the development of a hydration process and formation of cement-based productions, which happens with the consumption of free water. On the other hand, drying shrinkage of concrete occurs due to the water evaporation from the matrix and this kind of shrinkage can be pronounced if the curing condition is not properly provided [2,54]. Several studies have been conducted and proposed methods for reduction of shrinkage and its consequent cracks, such as microfibers, mineral and chemical admixtures, cement modification and control of the curing conditions [45,35].

Yalçınkaya and Yazıcı [69] in part of their study investigated the effect of relative humidity and temperature on the shrinkage of

high-performance concrete. They have observed in conditions with constant relative humidity at 50%, an increase in temperature from 20 °C to 40 °C not only can enhance the shrinkage strain values due to water evaporation, but also can accelerate its progress in the first hours. They have also observed that temperature rise, especially from 30 °C to 40 °C caused considerably more intense enhancement in water evaporation from the specimens compared to a temperature rise from 20 °C to 30 °C. It should be noted that although the high temperature in curing leads to high water evaporation from the surface of concrete, it also helps to speed up the hydration process, which contributes to more non-evaporable water or chemically bound water, therefore reducing in autogenous shrinkage [58]. Piasta and Zarzycki [48] conducted a study on the influence of w/c and paste volume of concrete on shrinkage. They stated that considering both effects of hydration degree development and increase in w/c, which leads to an increment of capillary porosity, the growth of shrinkage during drying can be explained because of excessive water loss through the surface of the concrete. Furthermore, the effect of paste volume can be notably enough to yield higher shrinkage values in specimens with lower w/c, but higher volume paste in comparison to specimens with higher w/c and lower paste volume.

Curing conditions, such as temperature and relative humidity, play a key role in improving the microstructure of concrete and minimizing the cracks that can speed up the process of penetration of aggressive ions, such as chloride, into concrete. In practice, concrete structures in harsh environments experience temperature and relative humidity different than that of the standard curing condition in the laboratory. Therefore, it seems vital to study the influence of different curing conditions on the penetration of chloride ions into concrete [18,31,43,17]. Jiang et al., [31] investigated the effects of curing temperature on the chloride migration coefficient with the use of the rapid chloride migration test (RCMT). They have observed in concrete without the pozzolan materials (ordinary concrete) an increase in temperature will decrease the migration coefficient (D_{RCMT}) values at early ages while at longer ages higher temperature contributes to a slight enhancement in D_{RCMT} values. Ogirigbo and Black [42,43] evaluated the effect of curing temperature at 20 °C and 38 °C on the penetration of chloride ions into concrete. They have observed that at the higher curing temperature (38 °C) bounded chloride content will grow. It is expected that free chloride ions in the pore solution decrease, thereby decreasing chloride penetration depth. Although, this trend was observed at early ages (14 days), long-term ages had a higher depth of penetration. This phenomenon was explained by the fact that, despite that the higher temperature increases the bound chloride, it makes the pore structure coarser, which in turn facilitates the penetration of chloride ions into concrete [39,44]. Caré [20] investigated the effect of w/c and different temperatures included 45 °C, 80 °C and 105 °C on chloride diffusion in cement paste. The results of this study showed that both increases in temperature and w/c ratio lead to growth in chloride diffusion values.

Almusallam [5] examined porosity of concrete specimens subjected to a temperature of 30 °C and 45 °C with different relative humidity of 25%, 50% and 90%. In this study, it was observed that at a constant temperature, an increase in curing relative humidities followed by a decrease in the magnitude of coarse pores (pore size more than 1000 Å) and total porosity of the specimens. Higher relative humidity can exclude the immoderate water evaporation from the structure of concrete by providing a higher volume of water vapor in the atmosphere, thereby helping the further hydration and production of C-S-H gel for making the microstructure denser.

The resistivity of concrete is an indicator of its resistance against the penetration of aggressive agents. Thus, it can be considered as a parameter to show durability. The microstructure of con-

crete is an important factor in the determination of electrical resistivity. In other words, connected micropores in the structure of concrete make the penetration of aggressive ions easier. Therefore, its electrical resistivity will be lower, and the probability of corrosion in concrete will be higher [22,38,40,26]. Environmental conditions, such as relative humidity and temperature, are factors that can significantly influence electrical resistivity. Sengul [53] observed that with an increase in the curing temperature, the electrical resistivity values decreased. He stated that temperature could considerably affect the mobility of electrons. In fact, with an increase in curing temperature, electrons move faster, which leads to a higher electrical conductivity and, as a result, lower electrical resistivity values [16,67]. In this study, specimens were cured in three different relative humidity levels, including water curing, air dried with 65% relative humidity and oven dried. It was observed that specimens that were cured in the oven had a greater electrical resistivity rather than air dried and water cured specimens, respectively.

Olsson et al. [46] also observed that higher relative humidity led to a higher conductivity of specimens, which means lower electrical resistivity values. They have also stated that at high relative humidity, mortars with a higher w/b had higher conductivity in comparison to mortars with lower w/b. However, at low relative humidity, there is a shift in trend, and mortars with a lower w/b demonstrated greater conductivity compared to mortars with higher w/b. They stated that more existing gel and more connected gel pores are the reason for this phenomenon.

Water sorptivity index (WSI) can represent the connectivity of pores in the microstructure. Inappropriate curing conditions, including relative humidity and temperature, can lead to greater WSI values. This means a higher penetration depth of water into concrete and poor durability properties [21,62]. Ogirigbo and Black [42,43] investigated the impact of temperature on sorptivity of concrete specimens that were cured at two curing temperatures of 20 °C and 38 °C and observed its great influence on sorptivity results. In fact, as it is reported in their studies, sorptivity enhances with temperature, which was consistent with the result of the recent research by Surana et al. [62]. They also stated that the porosity of concrete is not only controlled by the progress of the hydration degree, but also by the temperature. As a matter of fact, an increase in temperature can be detrimental to the microstructure of concrete and induces cracking that enhances the sorptivity values.

Castro et al. [21] investigated both effects of relative humidity and w/c on sorptivity values. Relative humidity values of 50%, 65% and 80% with w/c ratios of 0.35, 0.4, 0.45 and 0.5 were considered for investigation. In a constant w/c, an increase in relative humidity contributes to the reduction of water sorptivity. It should be noted that in lower relative humidity capillary pores of specimens are emptier in comparison to samples under higher relative humidity curing. Thus, they tend to absorb more water that leads to higher water sorptivity values. They have also reported that in a constant relative humidity increase in w/c leads to the growth of sorptivity values. This trend can be explained by the fact that increase in w/c enhances the porosity of specimens, thereby increase in water absorption and sorptivity can be observed.

Nie et al. [41], using BSE micrographs have observed that the microstructure of heat-cured mortars is porous with a heterogeneous dispensation of hydration products. In fact, owing to the higher temperature, clinker particles were surrounded by a more condensed shell of hydration products, which are an obstacle for reaching water to the surface of clinker particles and progress of hydration degree. Wei and Xiao [67], using of SEM photographs observed some cracks in the microstructure of concrete were cured at 30 °C in comparison to those were cured at 20 °C. They

accredited those cracks to the development of stress in specimens during formation of hydration products at a faster rate.

In this study, the effect of curing condition including relative humidity and temperature on mechanical and durability properties of mortar was investigated. Moreover, microstructural properties of samples with the use of thin sections were examined. Regression models for moisture loss and shrinkage were proposed in this research paper. Finally, Pearson correlation coefficient among mechanical and durability tests was calculated to assess their relationship.

2. Experimental program

2.1. Materials

The type I Portland cement was used for mixing the mortar samples. The physical properties of the cement are provided in Table 1. The oxide compositions of the Portland cement from the X-ray Fluorescence (XRF) test are listed in Table 2. The fine aggregate was a quartz sand with a fineness modulus and density of 2.26 and 2.52 g/cm³, respectively.

The mix proportions of mortar samples are listed in Table 3. Twelve mortar mixtures were proportioned with a particular sand/binder ratio of 2.75, according to the ASTM C109 standard. A polycarboxylic-ether type superplasticizer (SP) with a specific gravity of 1.12 was employed. The needed SP dosage to achieve the desired workability of 110 ± 5% in mixtures with 0.42 and 0.52 W/C was 0.78% and 0.45% (by mass), respectively [7]. In order to prepare samples with different temperatures, all materials in the mortar are equilibrated at different temperatures in advance.

To prepare mortar samples, the components were weighed. The SP was added into water, and then the cement was poured into this gel gradually. The gel, cement and remaining water continued to be mixed until the sand was added, and mixing continued until proper integrity was achieved. The final part was the mechanical mixing to ensure consistency of mixture design. Mortar specimens with dimensions of 5 cm were made per ASTM C 109 [7]. Specimens were cast in two layers, and the vibration table was used for entrapped air removal. Then, specimens were demolded after 24 h and cured in calcium hydroxide-saturated water at 24 ± 2 °C until testing time. River sand was used as the fine aggregate. The gradation was conducted in accordance with [11] as shown in Fig. 1. The water absorption, the fineness modulus, and specific gravity were 2.18%, 3.19, and 2415 kg/m³, respectively.

To study mechanical and durability effects of curing, several tests were conducted, which will be explained in following paragraphs. Each test, with associated standard, specimen's type, and dimensions, is tabulated in Table 4.

2.2. Test methods

2.2.1. Moisture retention test

The moisture retention test measured the moisture loss of a mortar specimen within a given period of time using a high-sensitivity scale. This test was carried out in accordance with the standard test, ASTM C 156 [8], which was related to the capability of a curing method to minimize evaporation. In this test, a cylindrical mold with a diameter of 30 cm and height of 7.5 cm height was used to measure moisture loss. The specimens' weight was recorded every two hours for 72 h. The moisture loss is defined relative to the total specimen weight. Since moisture loss was nearly constant after 24 h whether the concrete was cured or not, the most critical time to measure moisture loss measurement is in the first 24 h.

2.2.2. DC measurements

The DC or permittivity is measured by a percometer as shown in Fig. 2. The device has two segments: a probe, which was used to measure the DC, and the body of the instrument. The specifications of the percometer are listed in Table 5 [37]. The permittivity is measured by the change in the electrical capacity of the electrode (probe) due to the influence of the measured material at a frequency of 40–50 MHz. In this test, a diameter of 15 cm and a height of 5 cm was used to measure the DC changes [61].

In order to understand the character of the DC value distribution, based on the experiment's results, a modified Weibull distribution function is used. In probability theory and statistics, the Weibull distribution is a continuous probability distribution. The relation between the values of DC, measured in time from the final set is governed by the probabilistic relationship that is affected by time as well. The \overline{DC} is the mean value of measurement for each spot and is shown as:

$$\overline{DC} = \int_1^{\infty} p(x) dx$$

where $p(x)$ is the probability density function that is appropriate for DC data. This is, typically, a log-normal, Gumbel, or Weibull distribution, which is described below:

Table 1
Physical properties of Portland cement.

Blaine fineness (m ² /kg)	Density (g/cm ³)	Passing 45 mm,%	Setting time (min)	
			Initial	Final
2850	3.15	91.5	197	272

Table 2
Chemical analysis of Portland cement (wt.%).

Constituents	Oxides								LOI	Cement compounds			
	SiO ₂	Al ₂ O ₃	Fe ₂ O ₃	CaO	MgO	SO ₃	Na ₂ O	K ₂ O		C ₃ S	C ₂ S	C ₃ A	C ₄ AF
Percent content (%)	23.53	6.12	3.98	59.87	2.13	1.6	0.31	0.51	1.85	37.86	34.01	17.08	11.05

Table 3
Mixture designs and curing conditions.

Mixture designs	M1	M2	M3	M4	M5	M6	M7	M8	M9	M10	M11	M12
Relative humidity (%)	90	90	90	30	30	30	90	90	90	30	30	30
Temperature (°C)	25	45	65	25	45	65	25	45	65	25	45	65
Water-to-cement ratio (W/C)	0.42	0.42	0.42	0.42	0.42	0.42	0.52	0.52	0.52	0.52	0.52	0.52
Cement	569	569	569	569	569	569	569	569	569	569	569	569
Fine aggregate	1564	1564	1564	1564	1564	1564	1537	1537	1537	1537	1537	1537
Water	239	239	239	239	239	239	301.6	301.6	301.6	301.6	301.6	301.6

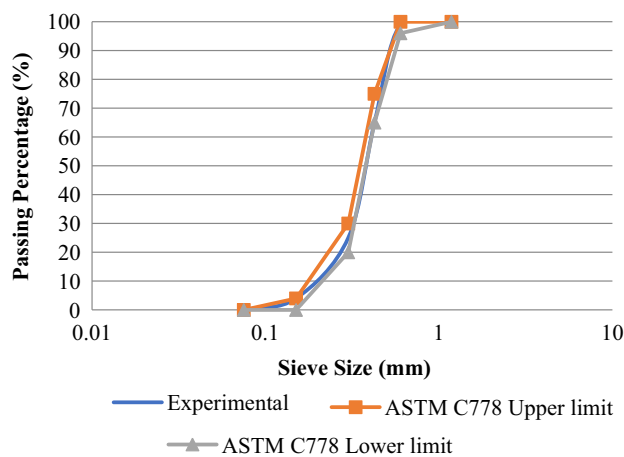


Fig. 1. Gradation of used sand.

Table 4
Type and number of specimens prepared and tested.

Test	Specimen Shape	Dimensions (mm)	Standard
Moisture retention test	Cylinder	300 × 75	ASTM C156
DC measurements	Cylinder	150 × 50	–
Compressive strength	Cube	50 × 50 × 50	ASTM C109
Shrinkage	Prism	50 × 50 × 200	ASTM C157
Water sorptivity index test	Cylinder	70 × 25	–
Rapid chloride migration test (RCMT)	Cylinder	100 × 200	ASTM C1202
Microscopical analysis	Slide	50 × 75	ASTM C856 and ASTM C457
Electrical resistivity test	Cylinder	100 × 200	ASTM C1760

$$p(x) = \gamma \lambda (\gamma x)^{\gamma-1} \exp[-(\lambda x)^\gamma]$$

In which the γ and λ are shape and scale parameters, respectively. The cumulative probability distribution function $P(x)$, which corresponds to the Weibull probability density function and fits through the data points relating DC and time from the final set, is indicated below:



Fig. 2. The Adek™ Percometer and the probe.

$$P(x) = 1 - \exp[-(\lambda x)^\gamma]$$

when $\gamma = 1$, the Weibull reduces to the exponential model, with $\alpha = 1/\lambda$. Depending on the value of the shape parameter γ , the Weibull model can empirically fit a wide range of data histogram shapes to appropriate mathematical equations. A modified Weibull distribution function shown in the following equation was used to generate regression curves for the DC measurements.

$$\bar{\epsilon}_r = \tau \left[1 - e^{-(\frac{t}{\beta})^\alpha} \right]$$

where

- $\bar{\epsilon}_r$ = the mean value,
- t = the elapsed time in hours,
- τ = the ultimate value of $\bar{\epsilon}_r$,
- β = the time factor that depends on the rate of application, and
- α = the rate factor that governs the rate of evaporation.

Linearizing the above equation, the exponential form is converted to a logarithmic equation. In the linearized form, the $\ln(t)$ is the variable, and α is the slope (rate parameter) representing the loss of moisture from the pavement surface indirectly.

2.2.3. Compressive strength test

Three 5 cm cubic mortar specimens were cast in accordance with ASTM C109 for each mixture [7]. The compressive strength test was conducted using a hydraulic testing machine under the loading rate of 1300 N/Sec at 3, 7 and 28 days of curing in accordance with ASTM C39 [6]. For each mixture design, the average was reported to evaluate the curing conditions.

Table 5
Specifications for the Percometer.

Measuring range					
Probe type	DC (ϵ_r)	Electrical conductivity, $\pm\mu S / m$	Temperature, °C	Accuracy of ϵ_r measuring	Recommended Application
Surface Probe	1 to 32	0 to 2000	-40 to +80	$\pm 0.1 + 1\%$	Laboratory use, Tube Suction Test

2.2.4. Shrinkage test

After hardening, concrete begins to shrink as water not consumed by cement hydration leaves the system. The shrinkage characteristics of a concrete mixture can be determined by ASTM C 157 [9]. This test method determines the change in length on drying of mortar bars containing cement that has been cured under different temperature and relative humidity values. The lengths and weights at 1, 3, 7, 14, 21 and 28 days age were recorded.

2.2.5. Water sorptivity index test

There are different methods to evaluate the absorption of mortar specimens. The sorptivity can be defined as the rate of movement of water through a porous material under capillary action. Each specimen consists of a 70 ± 2 mm diameter mortar disc with a thickness of 25 ± 2 mm cut in accordance with Concrete Durability Index Testing by Alexander et al. [3]. Preconditioned mortar samples were placed in saturated layers of absorbent material, and their mass gain was monitored at prescribed time intervals. The other sides of samples were sealed in order to measure uniaxial absorption. The WSI, which was interpreted as the rate of penetration of the water ($\text{mm}/\sqrt{\text{h}}$), was calculated by using the dimensions of the samples, porosity and the absorption rate. The typical range of results is $8.5 \text{ mm}/\sqrt{\text{h}}$ or less (for superior quality) to $15 \text{ mm}/\sqrt{\text{h}}$ or more (for poor quality) [28]. The sorptivity was calculated using following equation:

$$S = \frac{\Delta M_t}{t^{1/2}} \times \frac{d}{(M_{\text{sat}} - M_{\text{dry}})}$$

where

- S is the sorptivity in $\text{m}/\text{s}^{1/2}$,
- ΔM_t is the mass of water absorbed at time 't' in kg,
- T is the time in s,
- D is the specimen thickness in m,
- M_{sat} is the saturated mass in kg,
- M_{dry} is the initial mass in kg,
- $\frac{\Delta M_t}{t^{1/2}}$ is the slope of the best fit line for mass of water absorbed versus square root of time.

Directly after each curing treatment, the specimens should be placed in the oven at 50°C . Other surfaces (verticals) were covered with waterproof tape or epoxy paint to prevent penetration of water. The water sorptivity test should be conducted in a room in which the temperature is controlled at $23 \pm 2^\circ\text{C}$. The weight of absorbed water was measured after 30 min. At predetermined time intervals, the sample is weighed to determine the mass of water absorbed. Within 30 min after removing the specimen from the desiccator, the mass of the specimen to an accuracy of 0.01 g was determined and recorded as the dry mass at time zero. This mass should be determined after the method used to seal the sides of the specimens (either epoxy or tape) has been applied. The specimen was weighted at 3, 5, 7, 9, 12, 16, 20 and 25 min, after patting it once on the damp piece of absorbent paper [4]. The lower the WSI, the better is the potential durability of the concrete. A standard to set ranges for the WSI has not been published yet. However, an actual durability specification indicated the limits, which has found acceptance with authorities and consulting engineers. They reported WSI less than 9 is in acceptance zone and more than 15 is known as rejection [50].

2.2.6. Rapid chloride migration test (RCMT)

One of the primary purposes of RCMT is to determine the durability performance of the mortar. The test might examine the chloride resistivity of mortar mixtures at the age of 28 days. A 100×200 mm cylindrical specimen was cast for each mixture design and was divided into three disks with a thickness of 50 mm. These three disks were subjected to a 10% NaCl solution on one side and a 0.3 M NaOH solution on the other side. An external potential was applied across the specimen for 24 h to investigate the accelerated penetration of chloride ions. External potential will be adjusted based on the initial charges presented in NT build 492 [19]. Finally, the cylindrical slices were taken apart and axially split into two halves. To investigate the chloride penetration depth, a 0.1 M AgNO_3 solution was sprayed on the surface of the split halves for measuring the chloride ion penetration by observing the purple color through the chemical reaction. The average of the chloride migration coefficient was determined consistent with the NordTest Build 492 [19]. The chloride penetration was then used to calculate the migration coefficient according to [19,64,13]

$$D_{\text{nssm}} = \frac{0.0239(273 + T)L}{(U - 2)t} \left(x_d - 0.0238 \sqrt{\frac{(273 + T)Lx_d}{U - 2}} \right)$$

where "D_{nssm}" is non-steady state migration coefficient ($\times 10^{-12} \text{ m}^2/\text{s}$), "U" is the absolute value of the applied voltage, "T" is the average value of initial and final temperatures in the analyte solution ($^\circ\text{C}$), "L" is the thickness of the sample (mm), x_d is the average of penetration depths (mm), and "t" is the duration (hours) of the experiment.

2.2.7. Microscopical analysis (Thin sections)

Presence of voids, cracks, and other defects play an important role in determining the mechanical performance of the concrete. If a concrete surface is pre-damaged by microcrack formation in the near-surface area and exposed to open weathering, the capillary effect would increase the transfer of substances from the environment and increase the concrete volume, which can lead to several mechanisms capable of negatively influencing the durability of the concrete. To determine the effects of curing on concrete microstructure, concrete samples must be prepared and observed utilizing microscopy techniques. Petrography provides detailed compositional, textural, mineralogical, and microstructural properties of a mortar sample. Further information on the preparation of surfaces for microscopical analysis can be found in petrographic examination and determination of air-void systems references [10,12].

The most common types of mortar specimens observed in an optical microscope are thin sections. Included in these are picked grains, which are minute pieces of concrete extracted from a specimen, usually while observing it in the stereo microscope. These grains may be analyzed on the petrographic microscope using refractive index liquids or on the SEM. Thin sections are 20- μm -thick pieces of concrete bonded to a glass slide commonly using fluorescent dyed epoxy [32]. Thin sections are often required when examining concrete to allow for identification of components in the concrete microstructure. Then, the section is thinned by hand until the desired thickness and taper is achieved. The samples are shown in Fig. 3. The optical microscopy microanalysis was comparatively more useful than other tests in this study. The specimens selected for this study were chosen at the age of 30 days and were under two temperatures and three ambient relative rates.

2.2.8. Electrical resistivity

The electrical resistivity test was performed on water-saturated mortar cylinders of 100×200 mm in the lime water tank after curing periods of 7 and 28 days. The electrical resistivity is a function of moisture and electrolyte content of the pores in a mortar, which is measured based on AC impedance spectrometry using a resistance meter. These experiments have been done with the Wenner 4-probe meter. The likely difference and resulting current can be applied to find the electrical resistance. Four readings were obtained from the data logger for each cylinder specimen. The bulk resistivity was calculated as follows:

$$\rho = \frac{V}{I} \times (A/L) = R \times (A/L)$$

where ρ is the electrical resistivity ($\text{k}\Omega\cdot\text{cm}$), R is bulk electrical resistance ($\text{k}\Omega$), A is a cross-sectional area (cm^2), L is the distance between two electrodes (cm), I is measured current, and V is the voltage.

3. Results

3.1. Moisture loss

Ambient conditions might play an important role in the evaporation rates of cement mortar, regardless of mixture proportions. The duration of this test was 72 h, and the weight loss was recorded over time. In this study, the water retention capability of the specimens was tested under different relative humidity and temperature values as shown in Fig. 4. The contour plot represents the relationship between three variables and how temperature (y) and relative humidity (x) affect the moisture loss. This contour plot displays a two-dimensional view in which points that

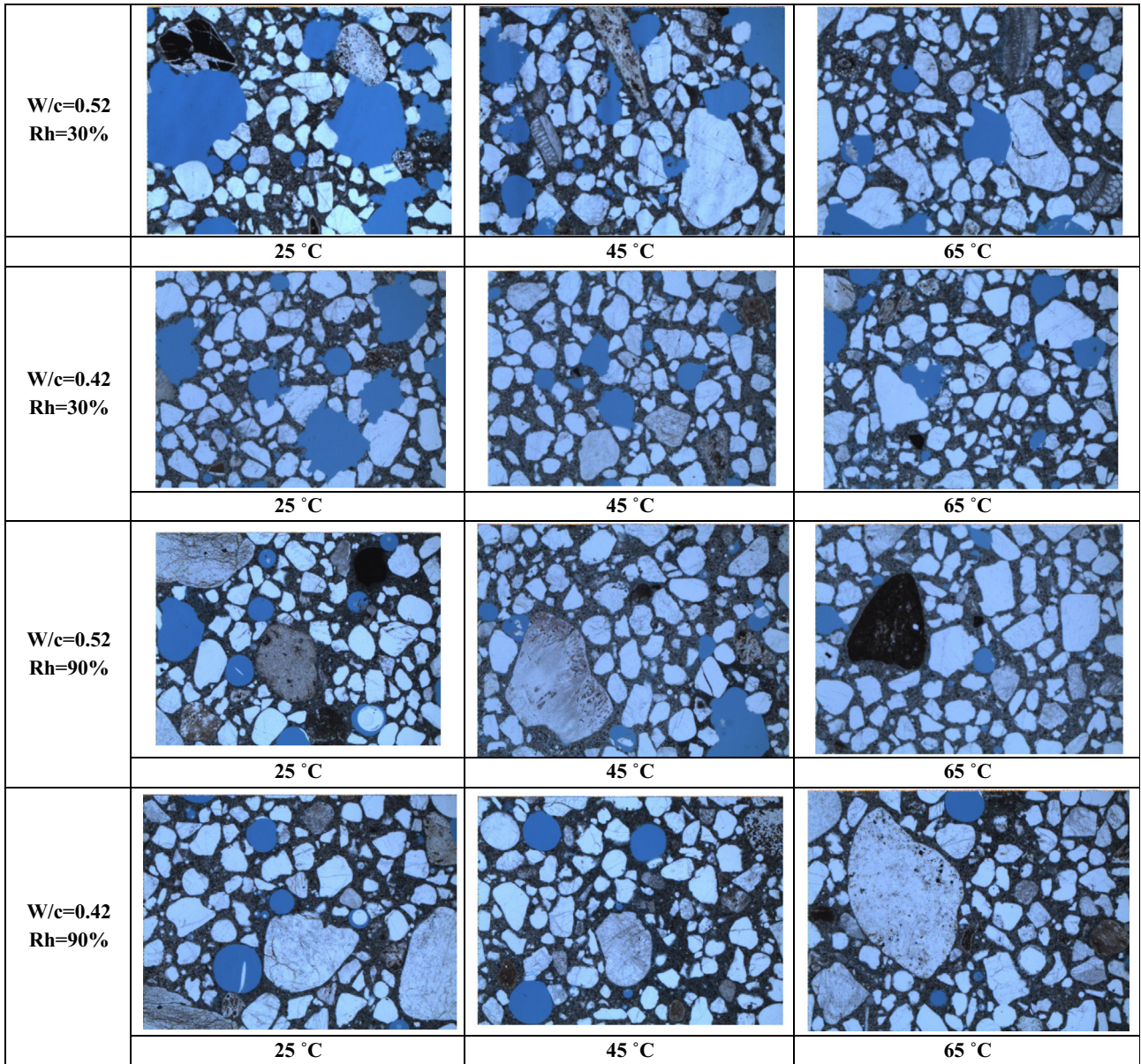


Fig. 3. Fluorescent epoxy impregnated thin sections prepared from mortar specimens.

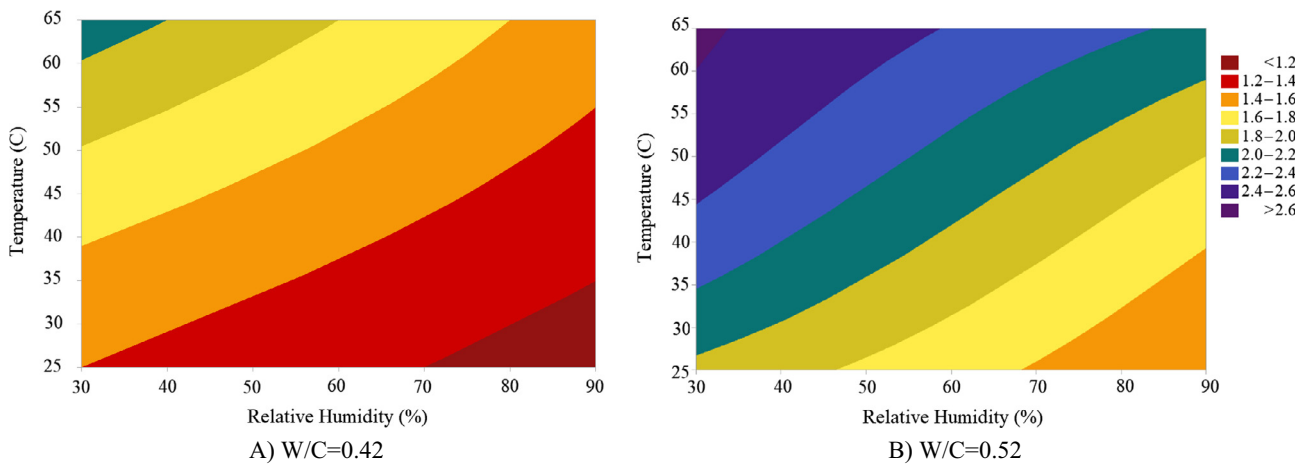


Fig. 4. The moisture loss trends at 72 h.

have the same response value are connected to produce contour lines.

In this graph, which consists of a spectrum of colors, red regions indicate lower moisture loss. These higher z-values seem to form a ridge running from the upper right of the graph to the middle left. The blue and purple parts represent higher moisture loss. It is well-known that if mortar is cured in a higher relative humidity, the moisture loss can be prevented significantly. This is achieved by blocking water transmission due to low moisture diffusion. Furthermore, an increase in temperature intensifies the rate of water evaporation and thus moisture loss, through the surface of mortar.

As displayed in Fig. 4, lower relative humidity and high temperature values increased the weight loss percentage. By considering the w/c, the higher w/c led to greater moisture loss because of the greater amount of evaporable water provided in the mortar [36]. For example, at the temperature of 65 °C and relative humidity of 65%, moisture loss in samples with w/c = 0.42 was 2.09%; however, this rate in mixtures with w/c = 0.52 was more than 2.6%. Fatuhi observed that specimens that were coated with a curing compound based on a hydrocarbon resin showed the best efficiency index in terms of water loss when exposed to the temperature of 25 °C and 50% of relative humidity [25]. When the temperature was raised to 60 °C and relative humidity reduced to 30%, the efficiency index decreased drastically.

In accordance with the obtained results, the moisture loss has a direct variation with temperature and inverse variation with relative humidity. Moreover, the variation with w/c was nonlinear, which caused the lines to be a curve instead of a straight line. Ishida et al. reported that a proposed model can simulate moisture loss behavior under varying temperature conditions and autogenous shrinkage in a closed system [29]. The relationship between the moisture loss percentage and curing conditions can be determined by

$$ML(\%) = \frac{a}{\left(\frac{V}{S}\right)_0 + b} \times \left(\frac{T}{T_0} + c\right) \times \left(1 + \frac{w}{cm}\right)^d$$

where ML is the moisture loss percentage compared to the initial age (%), $\frac{V}{S}$ is the volume-surface ratio (mm), T is the ambient temperature (C), R is the relative humidity (%), and the $\frac{w}{cm}$ is the water-to-cement-ratio. The $\left(\frac{V}{S}\right)_0$ is equal to 50 mm. The T_0 and h_0 , which are temperature and relative humidity references, are equal to one. The parameters a, b, c, and d are experimental coefficients. Accordingly, in this study, a regression model was developed to predict the moisture loss percentage [1]. This regression model is presented in:

$$ML(\%) = \frac{0.737}{\left(\frac{V}{S}\right)_0 + 5.763} \times \left(\frac{T}{T_0} + 2.302\right) \times \left(1 + \frac{w}{cm}\right)^{4.31}$$

The accuracy was $R^2 = 0.933$, which was calculated from the residual sum of squares divided by corrected sum of squares.

3.2. DC measurements

Research has indicated that DC is highly sensitive to the moisture content at the surface of concrete where DC measurements indicate strong relationships with the volumetric change in free water content. In early-age concrete, volumetric moisture content tends to be high due to incomplete hydration process, therefore DC measurements represent higher values. However, with time, due to moisture loss and hydration, the DC readings decline with a decrease of free water. In Fig. 5, the sensitivity of DC measurements to various curing practices is illustrated.

At an initial setting, the moisture content at the concrete surface was very high due to the presence of excessive free water. Thus, the DC measurements were correspondingly higher. Gradually, DC measurements began to decrease over a 96-h period, which also shows the progress of the hydration degree. After this period, the drying process begins when water is no longer available on the exposed surface. During the first drying stage, liquid water is present at the surface, which evaporates into the air. The rate of evaporation depends on the temperature, relative humidity and water content of the mixture design. It should be noted that the more ambient relative humidity, the lower the rate at which water will evaporate and the higher the DC values. As shown in Fig. 5A and B, at the same temperature, samples with a higher ambient relative humidity had higher DC values. The DC measurements of specimens treated with a similar relative humidity indicated similar sensitivity to temperature changes. As shown in Fig. 5A, the variation between different temperature regimens in a high ambient relative humidity (90%) was lower compared with a curing under a low relative humidity (30%). The reason might be attributed to the fact that higher relative humidity caused lower evaporation rates, and DC values are more likely not to change significantly.

The values of the analysis of variance (ANOVA) are shown in Table 6, which indicate whether the DC values difference between samples with different temperatures for both relative humidity values are significant. Based on a defined level of 0.05, when the significance factor is less than or equal to 0.05, a significant difference exists between different temperatures. Otherwise, samples with significance factor greater than 0.05 have a negligible difference [34,63]. Therefore, the temperature changes in a higher relative humidity (90%) would not change DC values substantially. While these variations in a lower relative humidity (30%) are meaningfully different.

It should be noted that an increase in temperature caused a reduction in DC values by two means. First, it increased the water evaporation rate, which directly reduced DC values. Second, a rise in temperature accelerated the hydration process and thus the consumption of free water and its change into bounded water. As can be seen in Fig. 5, an increase in temperature reduced DC values, regardless of the relative humidity and the w/c. It was detected that rates of change in DC values for specimens treated with higher temperature levels were greater than those treated with lower temperatures. In addition, trends exhibited that specimens with a higher w/c had higher DC measurements. The fitted regression parameters for all other sections are presented in Table 7. This information might help to differentiate moisture content for various mixture designs and curing conditions. Based on the regression parameters shown in Table 7, a higher moisture content is associated with a higher α . This could indicate that the curing practice applied on higher α samples had better quality and moisture retention capability, which resulted in a lower rate of the concrete surface moisture evaporation and corresponded to a lower decreasing rate of DC measurements.

3.3. Compressive strength

The average compressive strengths of specimens up to 28 days old are given in Fig. 6. As noted from the results, the compressive strength is developed in all mortar mixtures by aging. Moreover, in a constant relative humidity, the higher ambient temperature caused an increase in the compressive strength of specimens in initial ages (up to 7 days). However, specimens at the age of 28 days, which were cured under a higher temperature (65 °C) had lower compressive strength values as compared to specimens cured under a lower temperature. This matter must be related to the acceleration of production of C-S-H gel at early ages, which helps

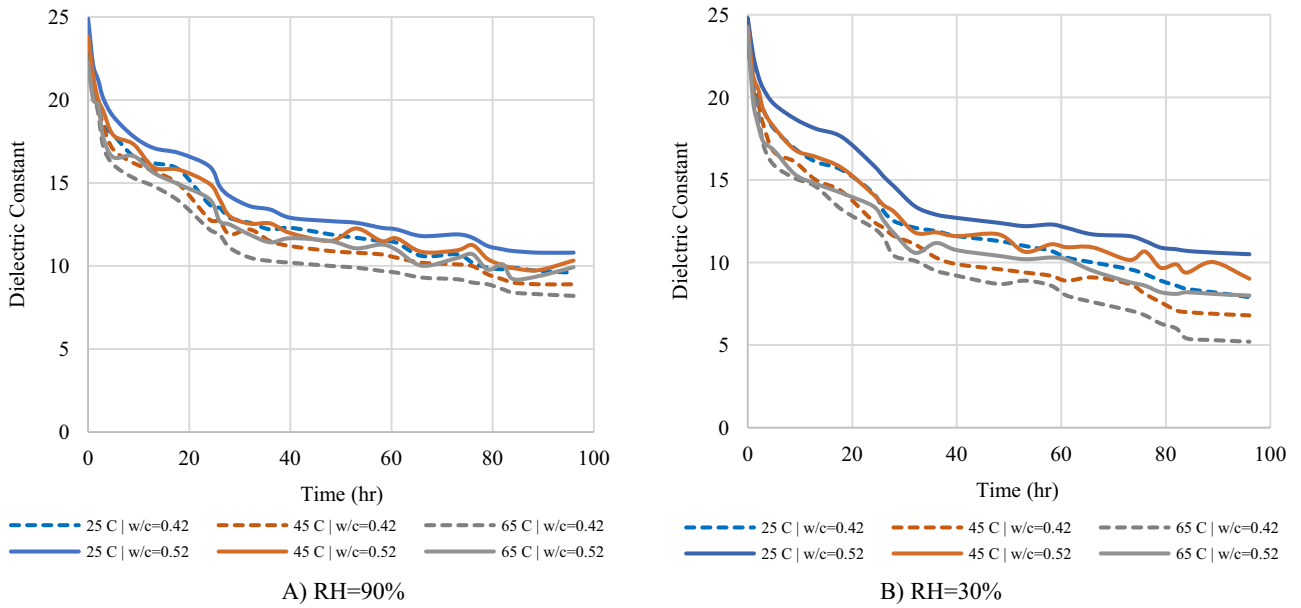


Fig. 5. DC measurements in different w/c, temperature and relative humidity levels.

Table 6
ANOVA results of compressive strength.

Curing types	RH = 90% w/c = 0.42			RH = 90% w/c = 0.52			RH = 30% w/c = 0.42			RH = 30% w/c = 0.52		
	25 °C	45 °C	65 °C	25 °C	45 °C	65 °C	25 °C	45 °C	65 °C	25 °C	45 °C	65 °C
Std. Dev.	–	0.997	0.979	–	0.854	0.652	–	0.124	0.038	–	0.004	0.001
Sig.	0.21	0.18	0.35	0.19	0.12	0.18	0.27	0.31	0.34	0.21	0.28	0.32

* The mean difference is significant at the 0.05 level.

Table 7
Regression parameters for the mixture designs.

Mixture designs	M1	M2	M3	M4	M5	M6	M7	M8	M9	M10	M11	M12
α	23.528	22.783	21.503	22.911	22.366	21.738	24.499	23.536	22.990	23.986	23.325	22.783
β	0.052	0.054	0.088	0.060	0.077	0.086	0.053	0.058	0.054	0.042	0.068	0.116
τ	0.346	0.375	0.362	0.418	0.445	0.496	0.326	0.334	0.336	0.385	0.355	0.335

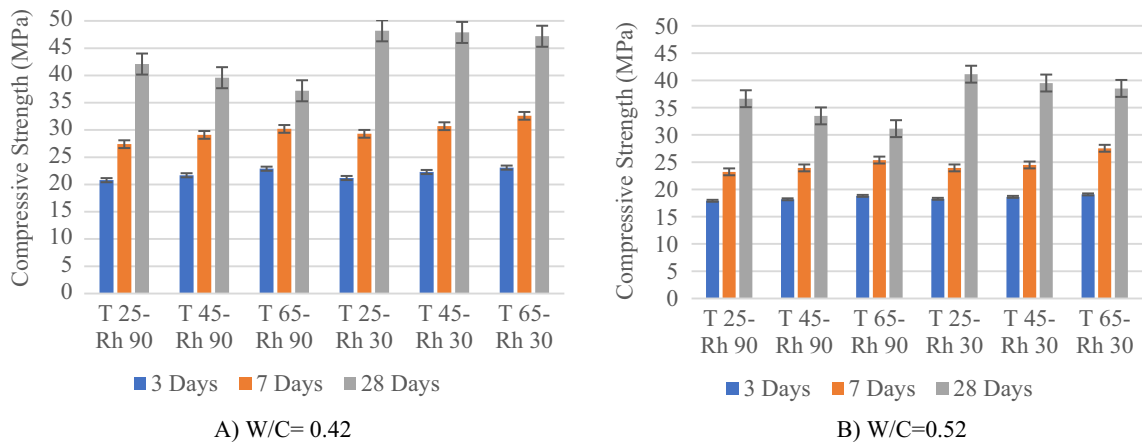


Fig. 6. Compressive strength results in 3, 7 and 28 days.

to develop compressive strength [51]. However, the heterogeneous distribution of C-S-H gel clusters leads to a porous microstructure of concrete that can adversely affect the results of this test. In this

study, the highest compressive strength was found at later ages and was obtained with w/c = 0.42. However, the highest early-aged compressive strength occurred at 65 °C at the same condi-

tions. There was a significant decline in the compressive strength by increasing the w/c. The standard deviations of samples were increased by growing the age of samples. Moreover, samples with a lower w/c (0.42) had higher standard deviations. For instance, the standard deviation of 3 days, 7 days and 28 days were 0.84, 1.59, and 4.32 for the w/c = 0.42, respectively. However, these values were obtained 0.39, 1.40, and 3.46 for the w/c = 0.52.

The concrete specimens were stronger at lower relative humidity levels and weaker at higher degrees of saturation. In the low degree of saturation (30%), the surface tension and compressive stress were increased due to the capillary suction effect. The reason for this is that the physical adsorption is the result of the forces of attraction and the molecules in the solid [72]. At higher relative humidity (90%), water starts to fill capillary pores in the concrete, which are outside the range of surface tension. Another reason for strength increasing might be that the water absorbed into gel pores lead to a transverse bursting effect in the solid matrix of the concrete, and this effect increases with an increase in the external compressive load. Similar results were reported in previous research studies [68,24].

3.4. Shrinkage

As shown in Fig. 7, the results indicate the shrinkage potential with elapsed time under different curing conditions. These moisture-induced volume changes are a characteristic of mortar. Since drying shrinkage is related to moisture loss from the mortar, it is influenced by external factors that affect drying and internal factors related to the concrete, such as temperature, ambient relative humidity and the w/c. As displayed in Fig. 7A and B, higher relative humidity levels may prevent moisture loss and mitigate adverse effects of this incident, such as shrinkage. Thus, specimens had lower shrinkage trends in higher moisture levels (90%). The drying shrinkage of mortar specimens was increased with increasing its water content. The variation in shrinkage with w/c may be clarified by the difference in types of water lost at the various stages of drying. In fact, an increase in the w/c not only provides greater free water content susceptible to evaporation but also causes its evaporation to be easier due to the more porous structure of the mortars [34]. In addition, shrinkage is associated with the modulus of elasticity. Samples with higher w/c had a lower strength and modulus of elasticity. Therefore, they had a greater tendency toward shrinkage. In this study, samples with higher w/c (0.52) had up to 16% higher shrinkage than lower w/c (0.42). Lower temperatures (25 °C) generally produced a decrease in drying shrinkage due to the slower evaporation. In contrast, water has high available thermal energy to drive evaporation at higher temperature (65 °C). The contradictory performance of a rise in temperature should be noted here. The direct effect of a rise in temperature is the enhancement of the water evaporation rate and an increase in shrinkage strain values. However, a rise in temperature simultaneously helps the water phase change from free water to bounded water by speeding up the hydration process. The development of hydration not only can prevent the evaporation of free water but can also enhance the compressive strength and modulus of elasticity at early ages, which can indirectly reduce the shrinkage strain values. In general, it seems a rise in temperature is more powerful in affecting water evaporation rate than changing free water into non-evaporable water.

The modification was used to calculate the shrinkage of normal strength concretes that are cured at different temperatures and exposed to a mean ambient relative humidity (30–100%). The models are valid for normal weight plain structural concrete having an average compressive strength in the range of 20 MPa < f_{cm28} < 90 MPa. The total shrinkage strains of concrete $\varepsilon_{sh}(t, t_c)$ may be calculated from:

$$\varepsilon_{sh}(t, t_c) = \varepsilon_{CSO} \beta_s(t - t_c) \beta_w \beta_T$$

where ε_{CSO} is the notional shrinkage coefficient, $\beta_s(t - t_c)$ is the coefficient describing the development of shrinkage with time of drying, t is the age of concrete (days) at the moment considered, t_c is the age of concrete at the beginning of drying (days), and $(t - t_c)$ is the duration of drying (days). The notional shrinkage coefficient may be obtained from:

$$\begin{aligned} \varepsilon_{CSO} &= \varepsilon_S(f_{cm28}) \beta_{RH,T}(h) \\ \varepsilon_S(f_{cm28}) &= \left[360 + 10 \beta_{SC} \left(9 - \frac{f_{cm28}}{f_{cm0}} \right) \right] \times 10^{-6} \\ \beta_{RH,T}(h) &= \beta_{RH}(h) \left[1 + \frac{a}{\left(1 - \frac{h}{h_0} \right)^b} \left(\frac{T}{T_0} \right) \right] \\ \beta_{RH}(h) &= c \left[1 - \left(\frac{h}{h_0} \right)^3 \right] \end{aligned}$$

where f_{cm28} is the mean compressive cylinder strength of concrete at the age of 28 days (MPa), f_{cm0} is equal to 10 MPa, β_{SC} is a coefficient that depends on the type of cement, h is the ambient relative humidity as a decimal, and h_0 is equal to one. Where $\beta_{RH,T}(h)$ is the relative humidity factor corrected with temperature. The T is the ambient temperature (°C) and T_0 is equal to one. The development of shrinkage with time is given by

$$\beta_s(t - t_c) = \left[\frac{\frac{t - t_c}{t_1}}{d \left[\frac{\frac{V}{S}}{\left(\frac{V}{S} \right)_0} \right]^2 + \frac{t - t_c}{t_1}} \right]^{0.5}$$

where $(t - t_c)$ is the duration of drying (days), t_1 is equal to one day, $\frac{V}{S}$ is the volume-surface ratio (mm), and $\left(\frac{V}{S} \right)_0$ is equal to 50 mm. The β_w and β_T are defined as following equations:

$$\begin{aligned} \beta_w &= \left(1 + \frac{w}{c} \right)^e \\ \beta_T &= \left(1 + \frac{f}{T} \right) \end{aligned}$$

In the above equations, a to f are empirical constants. Accordingly, in this study, a regression model is developed to predict shrinkage based on relative humidity, temperature, compressive cylinder strength of concrete at the age of 28 days, w/c and geometry (volume-surface ratio). This regression model is presented by the following equation:

$$\begin{aligned} \varepsilon_{sh}(t) &= 37.2 \times \left[1 - \left(\frac{h}{h_0} \right)^3 \right] \\ &\times \left[1 + \frac{63.94}{\left(1 - \frac{h}{h_0} \right)^{0.594}} \left(\frac{T}{T_0} \right) \right] \left[360 + 10 \left(9 - \frac{f_{cm28}}{f_{cm0}} \right) \right] \\ &\times \left[\frac{\frac{t - t_c}{t_1}}{57.39 \left[\frac{\frac{V}{S}}{\left(\frac{V}{S} \right)_0} \right]^2 + \frac{t - t_c}{t_1}} \right]^{0.5} \left(1 + \frac{w}{c} \right)^{2.297} \left(1 + \frac{171.8}{T} \right) \times 10^{-6} \\ R^2 &= 0.979 \end{aligned}$$

The accuracy was calculated from the residual sum of squares divided by the corrected sum of squares.

3.5. Water sorptivity index test

For measuring transport performance, the water absorption of the mortar samples was measured, as displayed in Fig. 8. Sorptivity

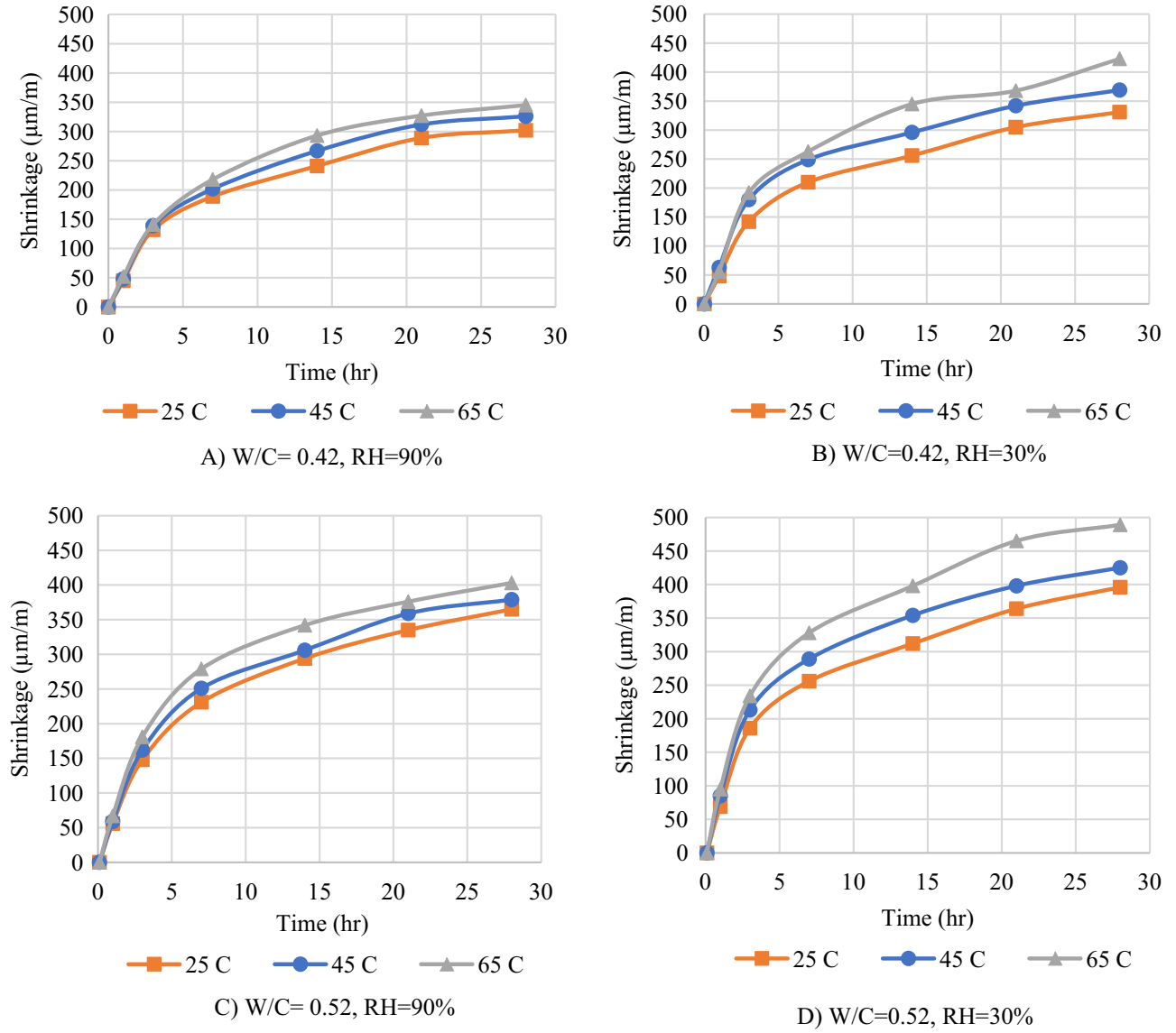


Fig. 7. Shrinkage test results under different temperature, relative humidity and w/c values.

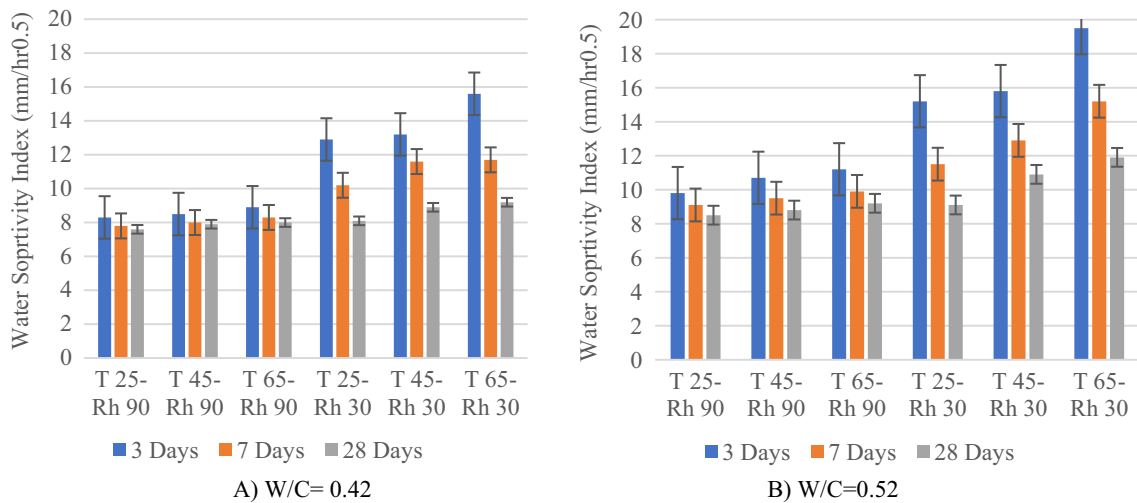


Fig. 8. WSI results in 4, 7 and 28 days.

can be defined as the rate of movement of water through a porous material under capillary action. A difference in trend was observed for the WSI due to sensitivity to the properties of the outer layers of the samples. The results showed that exposure to a temperature of 65 °C resulted in substantial increases in this index compared to other temperatures, which was considered as a poor quality index. The standard deviations of samples were decreased by increasing the age of samples. Moreover, samples with a lower w/c (0.42) had higher standard deviation values. For instance, the standard deviation of 3 days, 7 days and 28 days were 3.43, 2.15, and 1.23 for the w/c = 0.42, respectively. However, these values were obtained 2.80, 1.64, and 0.56 for the w/c = 0.52.

This general trend was observed for both mixtures with w/c of 0.42 and 0.52. The lower w/c (0.42) indicated better quality in the WSI because the specimen had a denser structure. Mortar samples that were cured for three days performed poorly, especially at a higher temperature (65 °C) while results obtained from specimens that were cured under 25 °C and 45 °C had similar or better performance. In later ages, the differences between the samples are less than early-aged ones. This indicated that an adequate curing period (28 days) ensured that the mortar had a sufficiently dense microstructure, enabling it to retain its moisture and benefit from the more rapid rates of hydration at higher temperatures. It should be noted that increasing the high temperature can bring about cracks in the microstructure of specimens, which leads to enhance water sorptivity values of the samples. This reason should be considered because the heterogeneous distribution of C-S-H gel during the hydration process under high temperature contributes to pore structure of the specimens, thereby increasing water sorptivity. The trends observed for samples cured under 90% relative humidity were almost identical to those of the 30%, with slightly better index values, especially at higher ages. It should be noted that differences in higher relative humidity values, regardless of temperature, age and w/c, were insignificant. Generally, specimens cured at 30% relative humidity had greater water sorptivity in comparison to the specimens cured at 90% relative humidity. This is because at lower relative humidity, capillary pores tend to absorb more water since they are emptier. An important observation that can be made from this investigation is that the sorptivity indexes of samples cured at higher temperatures, which showed poor performances, improved significantly when exposed to 90% relative humidity. This was most apparent for the WSI that higher relative humidities, to some extent, provide additional curing for concrete structures.

3.6. Rapid chloride migration test (RCMT)

The RCMT was carried out consistently with the NordTest Build 492 method at 28 days. Fig. 9 presents the non-steady state chloride migration coefficients calculated for mixtures under different curing conditions. Some properties of inner and outer portions of mortar samples are different due to the differences in their microstructure. This fact implies that the resistance against the intrusion of chloride ions was different for the various parts of concrete under different curing conditions. In this case, the outer parts of the sample were tested to minimize the differences.

The lower w/c decreased the migration coefficient and had better performance in durability improvement in the microstructure. The increasing rate of chloride resistivity is more perceptible at w/c of 0.52 than 0.42. It was observed that samples that were cured in a higher relative humidity (90%) showed lower migration coefficients. This improvement in durability is accredited to the development of the gel pore structure under sufficient moisture in the surrounding ambient conditions and to the elimination of excessive water evaporation from the surface of specimens. This observation was consistent with previous research studies [5]. Moreover, higher temperature (65 °C) reduced the chloride migration rates. This is attributed to the fact that the warmer ambient led to the acceleration of the cement hydration and greater magnitudes of reaction products, resulting in a denser microstructure. Therefore, the ability of higher temperature values to enhance the chloride ions' penetration resistivity of mortars was excellent. However, these results contradict previous studies' results at 28 days [20,41–43]. It was reported by other researchers that although an increase in temperature led to a decrease in migration coefficient at early ages, at longer ages there is a slight increase in migration coefficient values with an increase in temperature. Reduction in D_{RCM} values at early ages can be described by the accelerated hydration process and the denser structure of specimens due to more hydration products. On the other hand, at long-term ages, heterogeneous distribution of hydration products can surround un-hydrated cement particles and exclude them from the required moisture for the development of the hydration degree. As a result, incomplete hydration can contribute to performance deficiency and thereby enhancement in D_{RCM} values. In this study, regarding all other test results and it is anticipated that at the ages longer than 28 days, migration coefficient values increase with an increment in temperature.

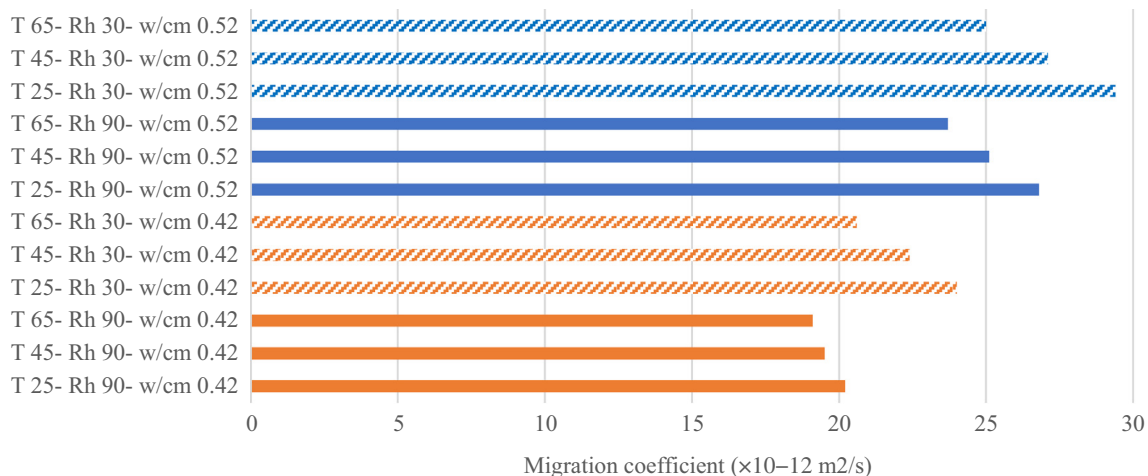


Fig. 9. Migration coefficients from RCMT at different temperature and relative humidity values.

3.7. Microscopical analysis (Thin Sections)

3.7.1. Air content

The images generated from each sample were analyzed with a microscopy imaging computer program (Zen lite) that would output the quantity of cracks found in the image field area. The quantitative analysis of the samples consisted of the identification and measurement of the cracks and crack density in the images. Images taken from central areas of the concrete matrix in the top-down form provided information related to the microstructure of the sampled concrete. An automatic mapping of the cracks was done in order to find out the total length of the microcracks and density per image area. The microcracks and voids were distinguished visually, and their corresponding lengths were measured using the image analysis software. The final outputs of the image analysis software are shown in Fig. 10. The sum of all air content in each image was computed. Lack of proper curing practice may increase the air content in concrete, since moisture evaporates easily from the concrete surface. Thus, the lower temperature and relative humidity caused higher air content. The induced shrinkage, moisture loss, and DC measurements were complied with the air content results.

Air content decreased with an increase in temperature. The hydration proceeds at a much slower rate when the concrete curing temperature is low. As the hydration of cement is accelerated with increased temperature, the air content was decreased. Orosz et al. reported thin section studies would help investigate the differences in pore structure due to different curing regimes [47]. They found higher curing temperatures would generate coarser pores and the distribution of capillary pores vs. air voids would be different depending on the curing regime. Goto and Roy also reported the same results. They measured the pore size distribution by mercury intrusion porosimetry at 27 °C and 60 °C. They reported the higher temperature had less air voids [27].

3.7.2. Types of voids

The overall void content in mortar is composed of three general types of voids: capillary voids, entrapped air voids, and water voids. Sample images were analyzed with a microscopy imaging computer program that maps the quantity and density of voids found in the image field area. The quantitative analysis of the samples consisted of the identification and measurement of the area of voids and their number density in the images [10]. Area of the voids is compared with the total area of the thin section studied, to get a percentage of void space, as shown in Fig. 11.

The smallest class of optically visible voids in the paste are the diverse sizes of capillaries. A few of the larger capillary voids may be seen at the higher magnifications used to determine the parameters of the void system, but they are generally not that large. Capillary voids are spaces formed by the shape of the hydrated cement gel structures and spaces left between the gel structures as water is used in the self-desiccation of the hydration process. They were occupied by water or gas when the mortar was fresh and are larger and more abundant in mortars with a high w/c. The magnitude of the capillary system is controlled by the w/c and the degree of maturity of the mortar samples. In samples under the same temperature and relative humidity conditions, those with w/c of 0.52 had the higher capillary voids compared to those with w/c of 0.42.

Samples which were cured under 90% relative humidity had lower capillary voids. As the cement hydrated, the water in the pores was used in the hydration. As the mortar samples matured, much of the capillary space became filled with the products of hydration and the products of any reactions occurring between the chemicals of the paste and the aggregate rocks. So, keeping moisture inside the body of concrete by increasing ambient relative humidity provided enough water in the pores for cement hydration. Therefore, less air content would support good maturity and less shrinkage. It is noteworthy that high relative humidity performs as a thick, wet blanket for mortars and doesn't let moisture escape.

Interconnected capillary voids are defined as the porous region of concrete in the thin section with more than 50% blue dye impregnated area, and size less than 100 μm as shown in Fig. 12. It is a weak zone rather than a well-defined void.

The irregularly sized air voids were spread throughout the mortar and had negative effects on product appearance and strength. This result was in accordance with compressive strength results.

3.7.3. Carbonation

The petrographic examination also provided information on the amount of carbonation of the sample. A better cured concrete tended to show less carbonation but this finding may depend on the effect carbonation has on the permeability of the surface concrete. In this study, a qualitative analysis of thin sections was done for the presence of carbonation. Carbonation starts at surface and diffuses into the concrete. As shown in Fig. 13, carbonation products may block the surface pores and lead to a slight decrease in permeability that may make it a viable parameter in which to assess curing quality [60]. All the samples showed carbonation on the surface mortar only.

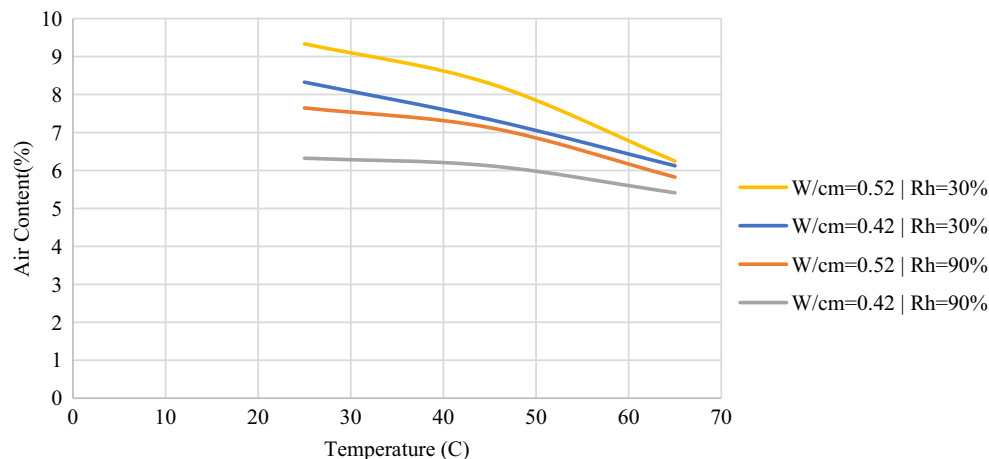


Fig. 10. Air content percentage of samples for different curing conditions.

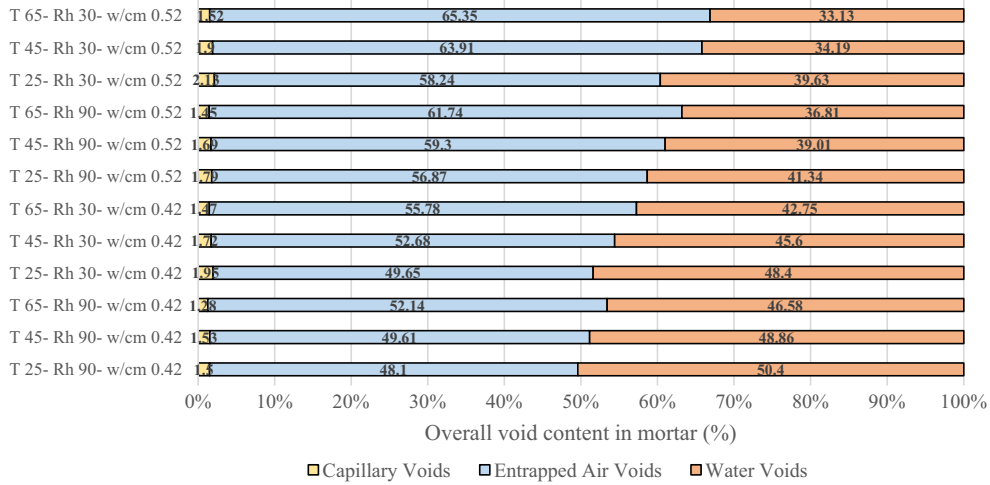


Fig. 11. The overall void content in mortar.

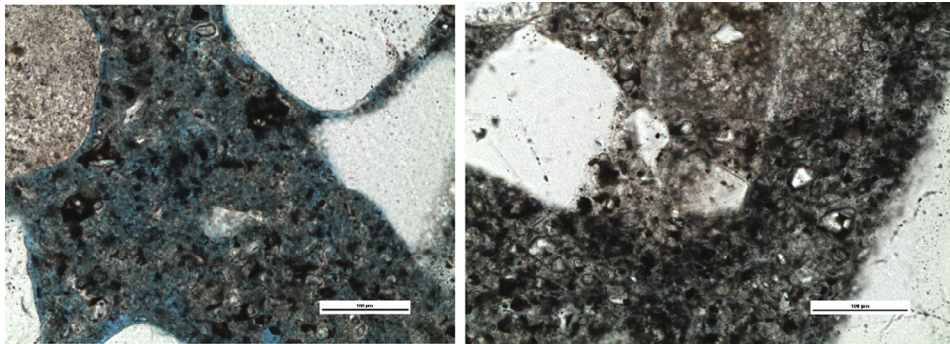


Fig. 12. Interconnected Capillary Voids (left) and Dense Paste (right).

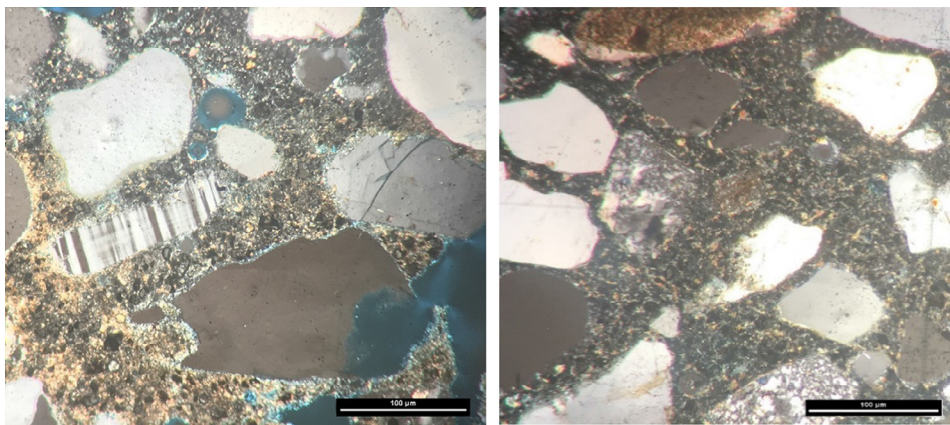


Fig. 13. Carbonated surface (left) as compared to uncarbonated interiors(right) of the concrete.

3.8. Electrical resistivity

The bulk electrical resistivity of mortar is a crucial factor that specifies the permeability of mortar to harmful agents. It had a significant correlation with the mortar pore structure and conductive ions. The electrical resistivity results for mixtures are shown in Fig. 14. The 28 days electrical resistivity had a higher standard deviation value.

It should be noted that the samples used in this evaluation were cured by keeping the samples in the constant conditions between

test measurements. The values of all samples increased with time. This high rate increase is attributed to hydration and porosity reduction. As can be seen in Fig. 14, at this age electrical resistivity values do not have a considerable difference, and curing conditions could not change test results significantly. However, the electrical resistivity values were improved in later ages. The higher temperature decreased the electrical resistivity and showed incremental trends. Although the hydration degree is higher at higher temperatures (65 °C) in comparison to the 45 °C and 25 °C, the hydration process and the microstructure is not the only factor that affects

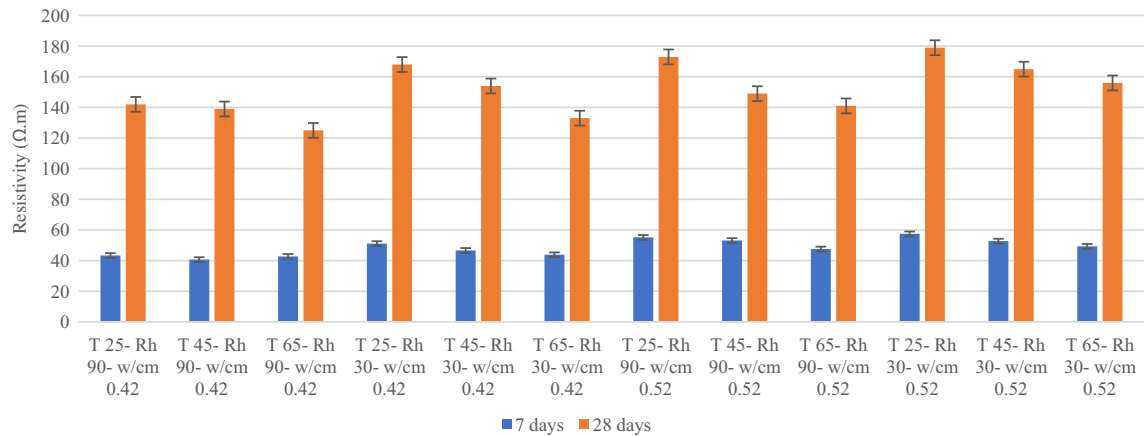


Fig. 14. Electrical resistivity of samples under different curing conditions.

Table 8

Correlation coefficients of mortar properties.

	Moisture Loss	DC	Compressive Strength	Shrinkage	Sorptivity	RCMT	Electrical Resistivity
Moisture Loss	1	–	–	–	–	–	–
DC	–0.143	1	–	–	–	–	–
Compressive Strength	–0.167	–0.535	1	–	–	–	–
Shrinkage	0.965	–0.105	–0.171	1	–	–	–
Sorptivity	0.202	–0.871	0.822	0.201	1	–	–
RCMT	0.514	0.815	–0.189	0.630	–0.770	1	–
Electrical Resistivity	0.106	0.835	0.101	0.142	–0.519	0.904	1

electrical resistivity values. In fact, a rise in temperature can outstandingly influence the mobility of electrons, which are responsible for the current through the pore solution. Thus, a rise in temperature enhanced the electrical conductivity of the specimens and contributed to lower electrical resistivity values. Another fact about electrical resistivity is its dependency on the ambient relative humidity. Based on the obtained results, samples had a lower electrical resistivity in a higher relative humidity (90%) than the lower one (30%). Regarding the fact that present ions in the pore solution are responsible for transmission of current, the presence of higher moisture content facilitated the transit of current through the pores, thereby enhancing the conductivity of the specimens and a reduction in electrical resistivity values.

3.9. Correlation coefficients among tests results

To examine the correlations of moisture loss, compressive strength, DC, sorptivity, RCMT and electrical resistivity, a correlation analysis is done by using the Pearson coefficient of the correlation function. The correlation coefficient (a value between -1 and $+1$) identifies how strongly two variables are linearly related to each other. A correlation coefficient of $+1$ indicates a perfect positive correlation (i.e., as variable X increases, variable Y increases or as variable X decreases, variable Y decreases). However, the correlation coefficient of -1 indicates a perfect negative correlation (i.e., as variable X increases, variable Y decrease or vice versa). This coefficient can be calculated by dividing the covariance of two variables by the product of their standard deviation. The statistical analysis is shown in Table 8.

Based on statistical perspective if the absolute value of an obtained correlation coefficient is between 0.7 and 0.9 there is a strong relationship between those variables. Furthermore, if such correlation is between 0.9 and 1 it is classified as a very strong correlation; whereas a correlation coefficient less than 0.5 classifies as a weak correlation [49]. Silva et al. reported the same range for the potency of the model. The correlation coefficients between the DC

and the sorptivity, the RCMT and the electrical resistivity can be classified as strong and very strong respectively. Shrinkage only had a very strong correlation with the moisture loss; however, the other mortar properties were not strongly correlated with shrinkage. The correlation between the compressive strength and the sorptivity is considered as a strong relationship. The correlation analysis between electrical resistivity with the moisture loss and the compressive strength were weak relationships. Although some studies found a good correlation between electrical resistivity and compressive strength, but it cannot always be true. Indeed, there are factors that can affect compressive strength while they have not any effect on electrical resistivity and vice versa. The strength of Interfacial Transition Zone (ITZ) has a great influence on compressive strength while it does not affect electrical resistivity of concrete. Moreover, a chemical compound of pore solution has a notable impact on electrical resistivity while it does not affect compressive strength. As a result, similar to Ramezaniyanpour et al. investigation not a reasonable correlation was found between these two values [52].

4. Conclusions

This paper investigated the influence of relative humidity and temperature curing and w/c on mechanical, durability and also microstructural properties of mortar. The following conclusions can be driven from this study:

1. Moisture loss had a direct variation with temperature owing to the increase in water evaporation rate with the rise of temperature. It has an inverse variation with relative humidity due to low moisture diffusion and protective performance of high relative humidity in evaporation of water through the specimens.
2. DC values which can represent free water content in the specimens are influenced by the curing relative humidity and temperature. High relative humidity reduced the water evaporation through the surface, and it caused DC values to

- be high. Two factors of increase in curing temperature and development of hydration process reduced free water content in the specimens, thereby reduction in DC values observed. It is worth mentioning that increase in temperature accelerated water evaporation and also hydration process, which both led to a reduction in free water content.
- Curing under higher temperatures accelerated the hydration and caused the heterogeneous distribution of hydration products. This condition makes the structure more porous and induced microcracks in the structure, which was responsible for increment in water sorptivity and reduction in compressive strength of specimens. In contrast, high relative humidity helped the progress of hydration degree and made the structure denser and as a result reduction in water sorptivity and increase in compressive strength was observed.
 - Rise in temperature caused evaporation of free water, which led to enhancement in shrinkage. But, it also changed the free water to bounded water through the acceleration of hydration process that can be influential in a slight reduction of shrinkage. However, in general, increase in temperature led to the growth of measured shrinkage. Furthermore, the positive impact of high relative humidity in the reduction of shrinkage through helping the prevention of water evaporation observed.
 - Rise in relative humidity through the providing sufficient moisture helped the hydration development, which led to denser microstructure and reduction in D_{RCM} values. Furthermore, the rise in temperature helped the acceleration of hydration and production of larger C-S-H magnitude that also led to a reduction of migration coefficient at the age of 28 days. However, it is anticipated that at longer ages, migration coefficient values increase with temperature rise due to the incomplete hydration that happened under high temperature.
 - At long-term ages rise in temperature accelerated mobility of electrons, therefore increased the conductivity of specimens and reduced their electrical resistivity. Moreover, a rise in relative humidity provided higher moisture and facilitated movement of ions through the microstructure of specimens and decreased their electrical resistivity values.
 - The microstructure study showed that the air content decreased with an increase in temperature. The magnitude of the capillary system is controlled by the w/c and the degree of maturity of the mortar samples. Lower w/c showed higher capillary voids compared. Moreover, samples which were cured under 90% relative humidity had lower capillary voids. A better cured concrete tended to show less carbonation.

References

- ACI-Committee209 (2008). 209R-92: Prediction of Creep, Shrinkage, and Temperature Effects in Concrete Structures (Reapproved 2008).
- S. Afzal, K. Shahzada, M. Ashraf, B. Alam, K. Khan, Autogenous shrinkage in high-performance concrete—a review, *Int. J. Adv. Struct. Geotech. Eng* 1 (01) (2012) 19–33.
- M. Alexander, Y. Ballim, J. Mackechnie, Concrete durability index testing manual, Res. Monograph 4 (1999).
- M.G. Alexander, Durability indexes and their use in concrete engineering, International RILEM Symposium on Concrete Science and Engineering: A Tribute to Arnon Bentur, RILEM Publications SARL, 2004.
- A.A. Almusallam, Effect of environmental conditions on the properties of fresh and hardened concrete, *Cem. Concr. Compos.* 23 (4) (2001) 353–361.
- ASTM-C39, Standard Test Method for Compressive Strength of Cylindrical Concrete Specimens, ASTM International, West Conshohocken, PA, 2017.
- ASTM-C109, Standard Test Method for Compressive Strength of Hydraulic Cement Mortars (Using 2-in. or [50-mm] Cube Specimens), ASTM International, West Conshohocken, PA, 2016.
- ASTM-C156, Standard Test Method for Water Loss [from a Mortar Specimen] Through Liquid Membrane-Forming Curing Compounds for Concrete, ASTM International, West Conshohocken, PA, 2017.
- ASTM-C157, Standard Test Method for Length Change of Hardened Hydraulic-Cement Mortar and Concrete, ASTM International, 2017.
- ASTM-C457, Standard Test Method for Microscopical Determination of Parameters of the Air-Void System in Hardened Concrete, ASTM International, West Conshohocken, PA, 2016.
- ASTM-C778, Standard Specification for Standard Sand, ASTM International, West Conshohocken, PA, 2017.
- ASTM-C856, Standard Practice for Petrographic Examination of Hardened Concrete, ASTM International, West Conshohocken, PA, 2017.
- ASTM-C1202, Standard Test Method for Electrical Indication of Concrete's Ability to Resist Chloride Ion Penetration, ASTM International, West Conshohocken, PA, 2012.
- C. Atiş, F. Özcan, A. Kılıç, O. Karahan, C. Bilim, M. Severcan, Influence of dry and wet curing conditions on compressive strength of silica fume concrete, *Build. Environ.* 40 (12) (2005) 1678–1683.
- M. Bakhshi, B. Mobasher, M. Zenouzi, Model for early-age rate of evaporation of cement-based materials, *J. Eng. Mech.* 138 (11) (2012) 1372–1380.
- I. Balafas, C. Burgoyne, Environmental effects on cover cracking due to corrosion, *Cem. Concr. Res.* 40 (9) (2010) 1429–1440.
- M. Balapour, E. Hajibandeh, A. Ramezani-pour, in: *Engineering Properties and Durability of Mortars Containing New Nano Rice Husk Ash (RHA)*. High Tech Concrete: Where Technology and Engineering Meet, Springer, 2018, pp. 199–206.
- M. Balapour, A. Ramezani-pour, E. Hajibandeh, An investigation on mechanical and durability properties of mortars containing nano and micro RHA, *Constr. Build. Mater.* 132 (2017) 470–477.
- N. Build, 492. Concrete, mortar and cement-based repair materials: chloride migration coefficient from non-steady-state migration experiments (1999).
- S. Care, Effect of temperature on porosity and on chloride diffusion in cement pastes, *Constr. Build. Mater.* 22 (7) (2008) 1560–1573.
- J. Castro, D. Bentz, J. Weiss, Effect of sample conditioning on the water absorption of concrete, *Cem. Concr. Compos.* 33 (8) (2011) 805–813.
- C.-T. Chen, J.-J. Chang, W.-C. Yeih, The effects of specimen parameters on the resistivity of concrete, *Constr. Build. Mater.* 71 (2014) 35–43.
- W. Chen, P. Shen, Z. Shui, Determination of water content in fresh concrete mix based on relative dielectric constant measurement, *Constr. Build. Mater.* 34 (2012) 306–312.
- X. Chen, W. Huang, J. Zhou, "Effect of moisture content on compressive and split tensile strength of concrete" (2012).
- N. Fattuhi, Curing compounds for fresh or hardened concrete, *Build. Environ.* 21 (2) (1986) 119–125.
- P. Gao, J. Wei, T. Zhang, J. Hu, Q. Yu, Modification of chloride diffusion coefficient of concrete based on the electrical conductivity of pore solution, *Constr. Build. Mater.* 145 (2017) 361–366.
- S. Goto, D.M. Roy, The effect of w/c ratio and curing temperature on the permeability of hardened cement paste, *Cem. Concr. Res.* 11 (4) (1981) 575–579.
- E. Griesel, M. Alexander, Effect of controlled environmental conditions on durability index parameters of portland cement concretes, *Cem. Concr. Aggregates* 23 (1) (2001) 44–49.
- T. Ishida, K. Maekawa, T. Kishi, Enhanced modeling of moisture equilibrium and transport in cementitious materials under arbitrary temperature and relative humidity history, *Cem. Concr. Res.* 37 (4) (2007) 565–578.
- C. Jabonero, S.W. Ryu, J.Y. Park, Y.-H. Cho, I.T. Kim, The analyses of environmental factors for curing concrete pavements inside tunnels, *KSCE J. Civ. Eng.* 3 (21) (2016) 766–773.
- P. Jiang, L. Jiang, J. Zha, Z. Song, Influence of temperature history on chloride diffusion in high volume fly ash concrete, *Constr. Build. Mater.* 144 (2017) 677–685.
- A. Joshaghani, The effect of trass and fly ash in minimizing alkali-carbonate reaction in concrete, *Constr. Build. Mater.* 150 (2017) 583–590.
- A. Joshaghani, M.A. Moeini, M. Balapour, Evaluation of incorporating metakaolin to evaluate durability and mechanical properties of concrete, *Adv. Concr. Constr.* 5 (3) (2017) 241–255.
- A. Joshaghani, M.A. Moeini, M. Balapour, A. Moazenian, Effects of supplementary cementitious materials on mechanical and durability properties of high-performance non-shrinking grout (HPNSG), *J. Sustainable Cem. Based Mater.* (2017) 1–19.
- A. Joshaghani, D.G. Zollinger, Concrete pavements curing evaluation with non-destructive tests, *Constr. Build. Mater.* (2017).
- J.-K. Kim, C.-S. Lee, Moisture diffusion of concrete considering self-desiccation at early ages, *Cem. Concr. Res.* 29 (12) (1999) 1921–1927.
- S.I. Lee, Development of Approach to Estimate Volume Fraction of Multiphase Material using Dielectrics, Texas A&M University, 2010.
- Q. Li, S. Xu, Q. Zeng, The effect of water saturation degree on the electrical properties of cement-based porous material, *Cem. Concr. Compos.* 70 (2016) 35–47.
- A. Lindvall, Chloride ingress data from field and laboratory exposure—Influence of salinity and temperature, *Cem. Concr. Compos.* 29 (2) (2007) 88–93.
- R.A. Medeiros-Junior, M.G. Lima, Electrical resistivity of unsaturated concrete using different types of cement, *Constr. Build. Mater.* 107 (2016) 11–16.
- S. Nie, S. Hu, F. Wang, P. Yuan, Y. Zhu, J. Ye, Y. Liu, Internal curing—A suitable method for improving the performance of heat-cured concrete, *Constr. Build. Mater.* 122 (2016) 294–301.
- O.R. Ogirigbo, L. Black, Influence of slag composition and temperature on the hydration and microstructure of slag blended cements, *Constr. Build. Mater.* 126 (2016) 496–507.

- [43] O.R. Ogrigbo, L. Black, Chloride binding and diffusion in slag blends: Influence of slag composition and temperature, *Constr. Build. Mater.* 149 (2017) 816–825.
- [44] B.H. Oh, S.Y. Jang, Effects of material and environmental parameters on chloride penetration profiles in concrete structures, *Cem. Concr. Res.* 37 (1) (2007) 47–53.
- [45] M.J. Oliveira, A.B. Ribeiro, F.G. Branco, Curing effect in the shrinkage of a lower strength self-compacting concrete, *Constr. Build. Mater.* 93 (2015) 1206–1215.
- [46] N. Olsson, V. Baroghel-Bouny, L.-O. Nilsson, M. Thiery, Non-saturated ion diffusion in concrete—a new approach to evaluate conductivity measurements, *Cem. Concr. Compos.* 40 (2013) 40–47.
- [47] K. Orosz, H. Hedlund, A. Cwirzen, Effects of variable curing temperatures on autogenous deformation of blended cement concretes, *Constr. Build. Mater.* 149 (2017) 474–480.
- [48] W. Piasta, B. Zarzycki, The effect of cement paste volume and w/c ratio on shrinkage strain, water absorption and compressive strength of high performance concrete, *Constr. Build. Mater.* 140 (2017) 395–402.
- [49] C.Y. Piaw, *Basic Research Statistics (Book 2)*, McGraw-Hill, Kuala, 2006.
- [50] B. Raath, Notes from a Workshop on Durability: 'Reinforced Concrete, Concrete Society of Southern Africa, Midrand, 2001.
- [51] A. Ramezani-pour, V. Malhotra, Effect of curing on the compressive strength, resistance to chloride-ion penetration and porosity of concretes incorporating slag, fly ash or silica fume, *Cem. Concr. Compos.* 17 (2) (1995) 125–133.
- [52] A.A. Ramezani-pour, A. Pilvar, M. Mahdikhani, F. Moodi, Practical evaluation of relationship between concrete resistivity, water penetration, rapid chloride penetration and compressive strength, *Constr. Build. Mater.* 25 (5) (2011) 2472–2479.
- [53] O. Sengul, Use of electrical resistivity as an indicator for durability, *Constr. Build. Mater.* 73 (2014) 434–441.
- [54] D. Shen, M. Wang, Y. Chen, T. Wang, J. Zhang, Prediction model for relative humidity of early-age internally cured concrete with pre-wetted lightweight aggregates, *Constr. Build. Mater.* 144 (2017) 717–727.
- [55] P. Shen, L. Lu, Y. He, F. Wang, S. Hu, Hydration monitoring and strength prediction of cement-based materials based on the dielectric properties, *Constr. Build. Mater.* 126 (2016) 179–189.
- [56] V. Slowik, M. Schmidt, R. Fritzsche, Capillary pressure in fresh cement-based materials and identification of the air entry value, *Cem. Concr. Compos.* 30 (7) (2008) 557–565.
- [57] S. Soldatov, M. Umminger, A. Heinzl, G. Link, B. Lepers, J. Jelonnek, Dielectric characterization of concrete at high temperatures, *Cem. Concr. Compos.* 73 (2016) 54–61.
- [58] A. Soliman, M. Nehdi, Effect of drying conditions on autogenous shrinkage in ultra-high performance concrete at early-age, *Mater. Struct.* 44 (5) (2011) 879–899.
- [59] M. Soutsos, G. Turu'allo, K. Owens, J. Kwasny, S. Barnett, P. Basheer, Maturity testing of lightweight self-compacting and vibrated concretes, *Constr. Build. Mater.* 47 (2013) 118–125.
- [60] D.A. St John, A.B. Poole, I. Sims, *Concrete petrography: a handbook of investigative techniques*, Arnold; Copublished in North, Central and South America by J. Wiley (1998).
- [61] Stephen Sebesta, W.C., Fan Gu, Soohyok Im, Alireza Joshaghani, Wenting Liu, Xue Luo, Robert Lytton, Bryan Wilson, Dan Zollinger, "Develop Nondestructive Rapid Pavement Quality Assurance/Quality Control Evaluation Test Methods and Supporting Technology." Texas Department of Transportation (TxDOT), Research and Technology Implementation Office (RTI) 0-6874 (2017).
- [62] S. Surana, R.G. Pillai, M. Santhanam, Performance evaluation of curing compounds using durability parameters, *Constr. Build. Mater.* 148 (2017) 538–547.
- [63] M. Tabatabaieian, A. Khaloo, A. Joshaghani, E. Hajibandeh, Experimental investigation on effects of hybrid fibers on rheological, mechanical, and durability properties of high-strength SCC, *Constr. Build. Mater.* 147 (2017) 497–509.
- [64] L. Tang, H. Sørensen, Precision of the Nordic test methods for measuring the chloride diffusion/migration coefficients of concrete, *Mater. Struct.* 34 (8) (2001) 479.
- [65] M. Velay-Lizancos, I. Martinez-Lage, M. Azenha, P. Vázquez-Burgo, Influence of temperature in the evolution of compressive strength and in its correlations with UPV in eco-concretes with recycled materials, *Constr. Build. Mater.* 124 (2016) 276–286.
- [66] G. Villain, A. Ihamouten, X. Dérobert, Determination of concrete water content by coupling electromagnetic methods: coaxial/cylindrical transition line with capacitive probes, *NDT & E Int.* 88 (2017) 59–70.
- [67] X. Wei, L. Xiao, Effect of temperature on the electrical resistivity of Portland cement pastes, *Adv. Cem. Res.* 24 (2) (2012) 69–76.
- [68] F. Wittmann, Surface tension shrinkage and strength of hardened cement paste, *Mater. Struct.* 1 (6) (1968) 547–552.
- [69] Ç. Yalçınkaya, H. Yazıcı, Effects of ambient temperature and relative humidity on early-age shrinkage of UHPC with high-volume mineral admixtures, *Constr. Build. Mater.* 144 (2017) 252–259.
- [70] S. Yehia, N. Qaddoumi, S. Farrag, L. Hamzeh, Investigation of concrete mix variations and environmental conditions on defect detection ability using GPR, *NDT & E Int.* 65 (2014) 35–46.
- [71] N. Yousefieh, A. Joshaghani, E. Hajibandeh, M. Shekarchi, Influence of fibers on drying shrinkage in restrained concrete, *Constr. Build. Mater.* 148 (2017) 833–845.
- [72] I. Yurtdas, N. Burlion, J.-F. Shao, A. Li, Evolution of the mechanical behaviour of a high performance self-compacting concrete under drying, *Cem. Concr. Compos.* 33 (3) (2011) 380–388.
- [73] Z. Zhang, B. Zhang, P. Yan, Hydration and microstructures of concrete containing raw or densified silica fume at different curing temperatures, *Constr. Build. Mater.* 121 (2016) 483–490.